Dynamic IMF production in ^{24}Mg+^{27}Al at intermediate energies

E.P. Prendergast [a], A. van den Brink [a], A.P. de Haas [a], R. Kamermans [a], P.G. Kuijer [a], C.T.A.M. de Laat [a], R.W. Ostendorf [b], E. Oti [a], A. Péghaire [c], R.J.M. Snellings [d]

[a] *Universiteit Utrecht/NIKHEF, P.O.Box 80.000, 3508 TA Utrecht, The Netherlands*
[b] *KVI, Zernikelaan 25, 9747 AA Groningen, The Netherlands*
[c] *GANIL, BP 5027, 14021 Caen Cedex, France*
[d] *LBNL, 1 Cyclotron Rd, MS 50A-1148 Berkeley, CA 94720, USA*

March 5, 1999

Abstract

The azimuthal correlations and polar-angle distributions of intermediate-mass fragments (IMFs) produced in $^{24}Mg+^{27}Al$ at 45 an 95 AMeV were studied. Measurements of α-particles and IMFs with $3 \leq Z \leq 8$ emmitted in the mid-rapidity region for mid-central events were compared to IQMD results and results from a static-source model. A maximum in the azimuthal-correlation function at 180° can not be described by independently emmitted particles. Momentum conservation of a small source as well as target-projectile correlations from IQMD show the same azimuthal correlations as the experimental data. The polar-angle distributions in the experimental data show a target-projectile seperation, thus giving evidence of dynamic IMF production.

Keywords: dynamic multifragmentation, IMF, IQMD, azimuthal correlations

The origin of IMF emission in heavy-ion reactions is a heavily debated subject in the field of intermediate-energy heavy-ion physics [1–12]. The nature of the production process will depend on the mass and energy of the colliding systems. In this letter measurements of the azimuthal correlations and polar-angle distributions are described for the ^{24}Mg+^{27}Al system at 45 and 95 AMeV. The latter energy is close to the balancing energy of approximately 110 AMeV [13]. Here it will be shown that the combination of these two methods gives conclusive evidence that IMF production for these small systems is a dynamic process, with no evidence of the formation of a mid-rapidity source.

The polar-angle distributions and the azimuthal correlations have been measured with the Huygens detectors [14] and the 'MUR' [15]. The Huygens detectors consist of a central time projection chamber (TPC) surrounded by a plastic scintillator barrel ($11^\circ \leq \theta_{\rm lab} \leq 78^\circ$) and a CsI(Tl) wall at backward angles ($121^\circ \leq \theta_{\rm lab} \leq 177^\circ$). The experimental data presented in this paper were measured in the TPC, which is highly symmetric in the azimuthal angle ϕ with an average accuracy of 3.1° [16]. The polar angle resolution ($\theta_{\rm lab}$) is better than 1° at 78° and better than 0.25° at 11°. The TPC was operated at a gas pressure of 150 mbar (CF_4) leading to energy thresholds from 5 AMeV for protons to 7 AMeV for boron. Particle identification was obtained using the E vs. dE technique, with E measured in the plastics and dE measured in the gas chamber. The ^{24}Mg ions were accelerated with the GANIL accelerator.

The azimuthal-correlation function is defined as:

$$C(\Delta\phi) = \frac{N_{\rm cor}(\Delta\phi)}{N_{\rm uncor}(\Delta\phi)}, \tag{1}$$

with $\Delta\phi$ the relative azimuthal angle between two particles, $N_{\rm cor}(\Delta\phi)$ the distribution of correlated fragment pairs and $N_{\rm uncor}(\Delta\phi)$ the distributions of uncorrelated pairs. Uncorrelated fragments are generated by mixing tracks from different events. Events are mixed which are of the same impact-parameter class and have the same fragment multiplicity. These generated mixed events are corrected for the detector granularity. The azimuthal-correlation analysis is done for mid-rapidity fragments only. These fragments are defined in terms of rapidity, Y as $|Y/Y_{\rm proj}| < 0.5$, with $Y_{\rm proj}$ the projectile rapidity in the centre-of-momentum frame.
Assuming that the charged particle multiplicity depends monotonically on the impact parameter [17, 18], three impact parameter classes were defined: peripheral, mid-central and central. IQMD [19] simulations combined with a GEANT [20] detector simulation showed that the central impact-parameter class was heavily polluted with mid-central events. Furthermore, the data showed that the charged-particle multiplicity of peripheral events was too low to warrant an analysis of these events. Therefore, only mid-central events, with $0.35 < b/b_{\rm max} < 0.7$ are presented.

The acceptance and efficiency of the Huygens set-up influences the observables, however, the effect on the azimuthal correlations is neglectable. Fig. 1 shows the IQMD results for IMFs with Z = 3-4 emitted at mid-rapidity at beam energies of 45 and 95 AMeV for mid-central events, before (open triangles) and after (filled triangles) the GEANT detector simulation. No detector effects are observed in the azimuthal-correlation function. The detector effects on the polar-angle distributions are stronger. These effects are presented in fig 2. The upper part of this figure shows the effects of the detector response for Z = 3-4 emitted at mid-rapidity at a beam energy of 45 and 95 AMeV. Although the detector effects are large, the distributions corrected for the detector effects compare well to the experimental data, as can be seen in the lower

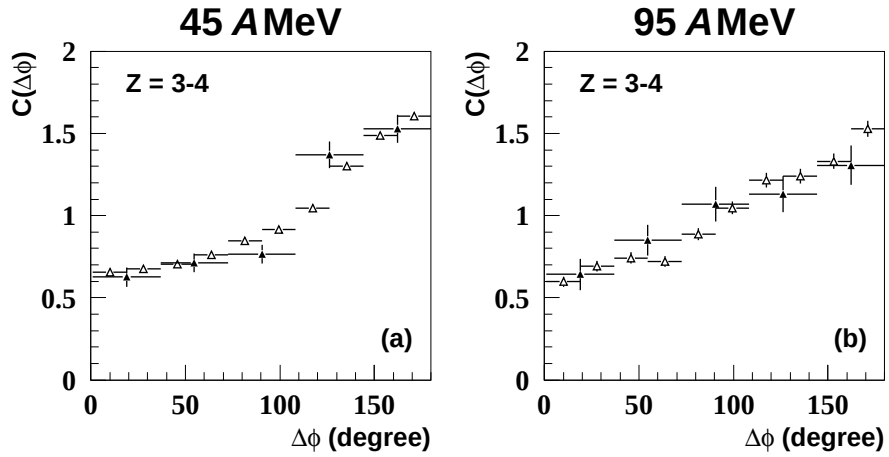

Figure 1: Azimuthal correlations of IQMD events of IMFs with Z = 3-4 emitted at mid-rapidity at a beam energy of 45 and 95 AMeV for mid-central events. The IQMD data before (open triangles) and after (filled triangles) the GEANT detector simulation are compared.

part of the same figure. Therefore, also for the polar-angle distributions, the detector effects are well under control.

Two models have been used to investigate the reaction mechanism for ^{24}Mg+^{27}Al at 45 and 95 AMeV. Firstly, the IQMD model, which gives a dynamic description of the heavy-ion collision. In total 600.000 IQMD events were generated at a beam energy of 45 AMeV and 800.000 events at a beam energy of 95 AMeV. Secondly, because the maximum at 180° in the azimuthal-distribution function could also be due to momentum conservation of a small decaying source [21–23], a static-source model was used to describe the measured distributions. The decaying mid-rapidity source is described by a model undergoing prompt multifragmentation [24]. In this model the Coulomb interaction is neglected and the multifragmentation process is governed by phase space only. The excitation energy for the source was taken to be the average centre-of-mass energy per nucleon, i.e. 11 AMeV and 23 AMeV for beam energies of 45 AMeV and 95 AMeV, respectively.

Fig. 3 gives the comparison of the experimental data (filled squares) with the results of IQMD (filled triangles) and the static-source simulations (open crosses). Since the detector does not influence the azimuthal distributions, the azimuthal distributions of IQMD without the GEANT detector simulation are shown. In figures 3b and 3e also the uncorrelated azimuthal distribution is shown (open circles), these distributions are flat, except for the dip at small angles due to the detector granularity. Only for Z = 2 the results are slightly

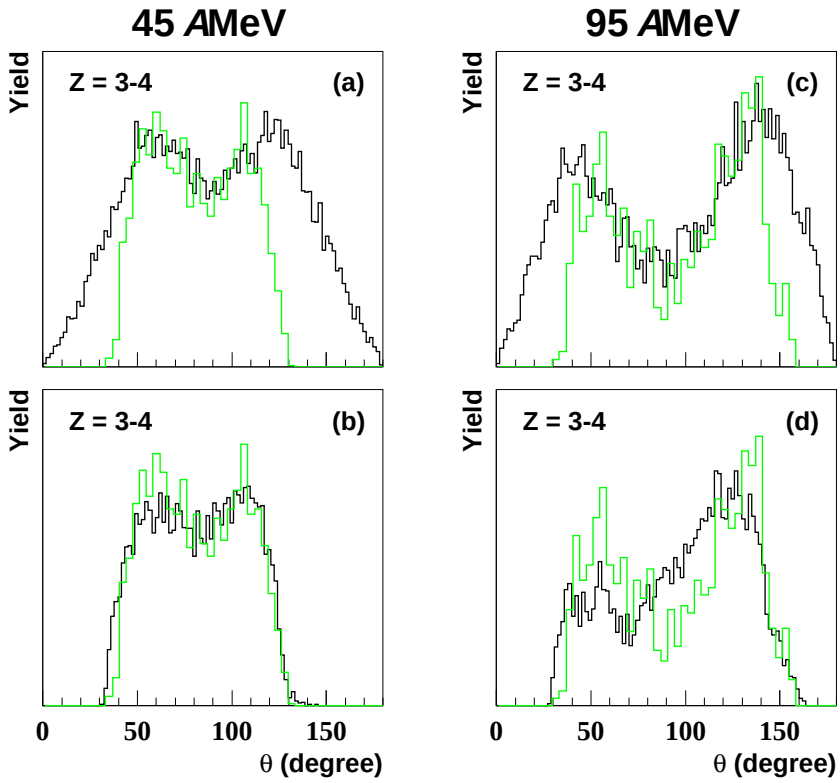

Figure 2: Polar-angle distributions of Z = 3-4 emitted at mid-rapidity at a beam energy of 45 AMeV in figures (a) and (b) and 95 AMeV in figures (c) and (d) for mid-central events. In (a) and (c) the distributions are shown for IQMD results before (black line) and after the GEANT detector simulation (grey line). Figures (b) and (d) show the experimental data (black line) and the IQMD results after GEANT (grey line). The distributions in (b) and (d) have been normalised to the integrated area of the plots. In (a) the plots have been normalised to the integrated area between 55° and 110° and in (c) the normalisation was done for the area between 55° and 140°.

different for IQMD and the experimental data. This is believed to be due to the different production process for $Z = 2$ than the heavier IMFs, which is not incorporated in IQMD. All other distributions of the experimental data and IQMD are in good agreement. The static-source simulations were fitted to the experimentally measured azimuthal distributions. For the $Z = 2$ data the mass of the source is 32, for Z = 3-4 the mass is 36 and for Z = 5-8 the mass is 40 amu. These values are the same for both beam energies. The mass distribution of the (other) decay products, i.e. the number of emitted particles, has very little influence on the distributions. Except for the $Z = 2$ results,

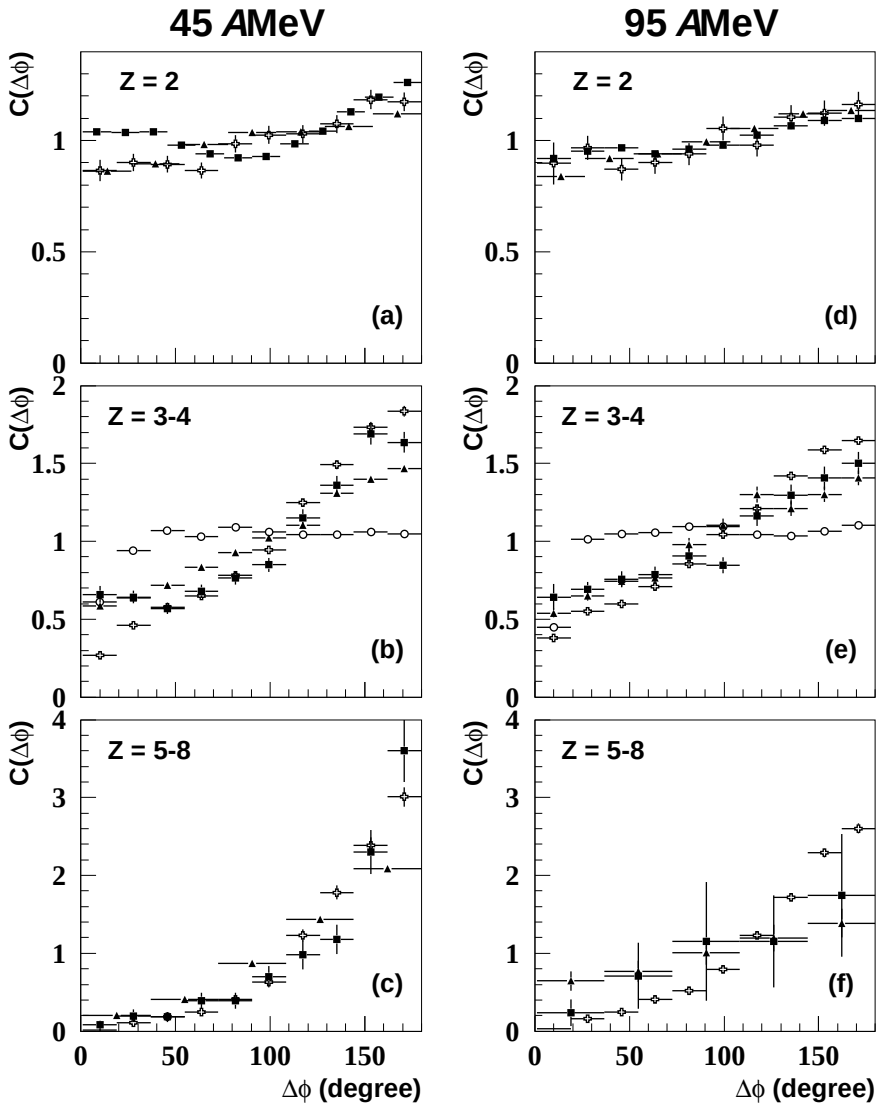

Figure 3: Azimuthal correlations of the experimental data (filled squares), the IQMD events (filled triangles) and the static-source events processed by GEANT (open crosses). All events are mid-central and the IMFs are emitted in the mid-rapidity area, the fragment charge is indicated in the top-left corner of each plot. In figures (b) and (e) also the uncorrelated azimuthal distributions are shown (open circles).

the decaying static-source distributions are in agreement with the experimental

data, although the levelling off of the experimental data (and the IQMD data) at small angles is not reproduced. The static-source model and IQMD give an equally good description of the measured azimuthal distributions. However, the pronounced maxima at 180° in the azimuthal-correlation functions exclude independently emmitted fragments from a single mid-rapidity source [25–28]. Coulomb repulsion [27, 29] is also not responsible for these maxima in the azimuthal distributions [30].

Although it is not possible to distinguish the two described models by studying the azimuthal correlations, the polar-angle distributions should be able to make a distinction [30]. Any decaying source at mid-rapidity will have a maximum in these distributions at 90°, whereas the polar-angle distributions of IQMD show a minimum at 90° flanked by two maxima, which are remnants of the target and the projectile and are therefore called target-like and projectile-like [30, 31]. This is a fundamental difference between the two models; an equilibrated decaying source has lost by definition all information about its initial state, whereas IQMD shows a strong initial-final state correlation. Fig. 4 shows the polar-angle distribution at mid-rapidity for the different fragments at the two beam energies. On the left-hand side the IQMD results after GEANT (grey line) are compared to the measured distributions (black line), on the right-hand side the measured distributions (black line) are shown with the static-source results (grey line). For 45 AMeV the IQMD results nicely describe the measured data. For Z = 3-4, fig. 4c and 4d clearly show that the experiment and IQMD are in agreement and that the static-source model fails to describe the measurement. For heavy fragments, fig. 4e and fig. 4f the projectile-like and target-like maxima fall outside the experimentally accessible domain, despite this, the measurement is in agreement with IQMD and is different from the static-source model. The figures 4a and 4b for the $Z = 2$ distributions show no significant difference between IQMD and the static-source model. The data, however, seems to indicate target-like and projectile-like maxima. As in the azimuthal-correlation function this difference between the experimental data and IQMD is probably due to the contrinution of a different production process for $Z = 2$. The 95 AMeV distributions show essentially the same results as the 45 AMeV distributions. The experiment is well described by IQMD and the static-source model fails to describe the data. For $Z = 2$ the data in fig. 4g show definite target-like and projectile-like maxima in both the measured data and IQMD. The static-source model in fig. 4h shows a maximum where both other distributions show a minimum. This is also the case in fig. 4j for Z = 3-4. Statistics do not allow for a comparison of the Z = 5-8 data, for completeness they are shown in figures 4k and 4l.

These results, of the azimuthal distribution function of mid-rapidity particles in conjunction with the polar-angle distributions, show that the IMF emission in nuclear collisions of ^{24}Mg+^{27}Al at 45 AMeV and 95 AMeV is governed by dynamic processes with no experimental evidence of a mid-rapidity source. The maxima in the azimuthal distributions were shown to be due to the correlations

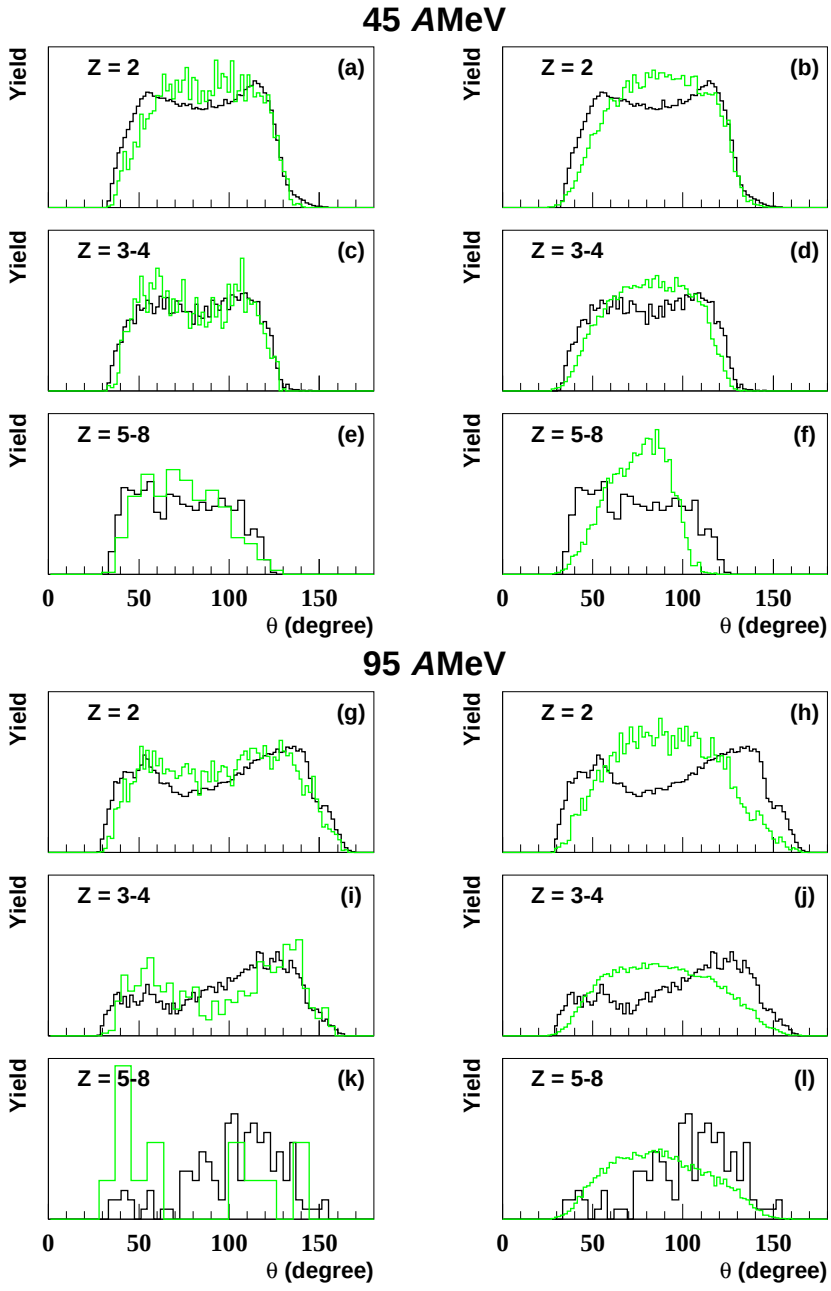

Figure 4: Polar-angle distributions for the experimental data (black lines) and on the left-hand side IQMD data after GEANT (grey lines) and on the right the static-source data (grey lines). The fragment charge is indicated in the top-left corner of each plot.

between target-like and projectile-like fragments. Nuclei of the small system studied here are not able to form a compound system. However, increasing the size of one of the nuclei, the azimuthal distributions start to show a more symmetric shape [21, 23]. This could indicate that pressure from the surrounding nuclear matter forces the creation of a compound system. However, as was shown above, very different scenarios can lead to a similar azimuthal-correlation function.

We would like to thank the colleagues at GANIL for their valuable help and the LPC for making the 'MUR' available. We would also like to thank C. Hartnack for providing the IQMD code. This work was performed as part of the 'Stichting voor Fundamenteel Onderzoek der Materie' (FOM) with financial support from the 'Nederlandse Organisatie voor Wetenschappelijk Onderzoek' (NWO).

References

[1] A.S. Botvina and D.H.E. Gross, Phys. Rev. C58 (1998) 23.

[2] J. Tõke and W.U. Schröder, preprint cern-th/9807066 (1998).

[3] A.S. Botvina and D.H.E. Gross, preprint CERN, nucl-th/9808004 (1998).

[4] L. Phair *et al.*, Phys. Rev. Let. 75 (1995) 213.

[5] M. D'Agostino *et al.*, Phys. Let. B371 (1996) 175.

[6] N. Marie *et al.*, Phys. Let. B391 (1997) 15.

[7] L. Beaulieu *et al.*, Phys. Rev. Let. 81 (1998) 770.

[8] L. Phair *et al.*, preprint LBNL-41893 (1998), sub. Phys. Rev. C.

[9] J. Tõke *et al.*, Phys. Rev. Let. 77 (1996) 3514.

[10] J. Tõke *et al.*, Phys. Rev. C56 (1997) 1683.

[11] M.F. Rivet *et al.*, preprint GANIL P9815 (1998), acc. Phys. Let. B.

[12] O. Tirel *et al.*, preprint GANIL P9826 (1998).

[13] G.D. Westfall *et al.*, Phys. Rev. Let. 71 (1993) 1986.

[14] T.M.V. Bootsma *et al.*, Nucl. Instr. and Meth. A349 (1994) 204.

[15] G.Bizard *et al.*, Nucl. Instr. and Meth A244 (1986) 483.

[16] E.P. Prendergast, Ph.D. Thesis, Universiteit Utrecht (1999), ISBN 90-393-1830-1.

[17] C. Cavata *et al.*, Phys. Rev. C42 (1990) 1760.

[18] L. Phair *et al.*, Nucl. Phys. A548 (1992) 489.

[19] J. Aichelin, Phys. Rep. 202 (1991) 233.

[20] GEANT 3.21, CERN Program library long writeup W5013.

[21] C.B. Chitwood *et al.*, Phys. Rev. C34 (1989) 858.

[22] T. Ethvignot *et al.*, Phys. Rev. C47 (1993) 2099.

[23] T. Ethvignot *et al.*, Phys. Rev. C48 (1993) 618.

[24] F. James, CERN report 68-15 (1968).

[25] R.A. Lacey *et al.*, Phys. Rev. Let. 70 (1993) 1224.

[26] S. Wang *et al.*, Phys. Rev. C44 (1991) 1091.

[27] L. Phair *et al.*, Phys. Rev. Let. 77 (1996) 822.

[28] W.Q. Shen *et al.*, Phys. Rev. C57 (1998) 1508.

[29] T.M. Hamilton *et al.*, Phys. Rev. C53 (1996) 53.

[30] R.J.M. Snelling *et al.*, Phys. Let. B426 (1998) 263.

[31] P.-B. Gossiaux and J. Aichelin, Phys. Rev. C56 (1997) 2109.